eman ta zabal zazu
Universidad del País Vasco
Euskal Herriko Unibertsitatea
ZIENTZIA ETA TEKNOLOGIA FAKULTATEA
FACULTAD DE CIENCIA Y TECNOLOGÍA

Gradu Amaierako Lana

Biokimika eta Biologia Molekularreko Gradua

The role of VAV3 in resistance to breast cancer endocrine therapy

Egilea:

Maria Hernandez Arregi

Zuzendaria:

Dra. Sara Manzano Figueroa (IIS Biodonostia)

Tutorea:

Dr. Arkaitz Carracedo

Leioa, 2023ko otsailaren 13a

TABLE OF CONTENTS

Acknowledgements:

I would like to express my greatest appreciation to Dr Sara Manzano not only for showing me how to organise and conduct laboratory experiments, but also for always having a positive and supportive attitude towards me. I would also like to thank everyone in the laboratory for being a part of this journey with me. Finally, I want to show my gratitude to Dr María M. Caffarel for giving me this opportunity and for being a clear example of motivation and perseverance, as well as to Dr Arkaitz Carracedo for recommending me this amazing group and always being willing to help me with bureaucratic issues.

1. INTRODUCTION

Breast cancer

Breast cancer (BC) is the most commonly occurring cancer in women and the most prevalent cancer overall (Winters et al., 2017). Indeed, data indicate that 1 in 8-10 women will suffer from it throughout their lives and 30% of BC patients will die from this disease. The highest incidence rates are observed in developed countries, mainly due to exposure to environmental and lifestyle risk factors. Last years' data demonstrate that death rates are declining, but not equally everywhere. Developing countries are the ones with the highest mortality rates due to the lack of resources for preventive screening for early detection and adequate treatment supplies (Loibl et al., 2021).

BC can be classified into subtypes according to different criteria, but the most clinically relevant are the classifications determined by immunohistochemistry (IHC) and by molecular features (Harbeck et al., 2019). By IHC, BC is clinically divided into three groups: Hormone receptor (oestrogen and progesterone receptor, abbreviated as ER and PR) -positive (HR^+, also denoted as ER^+), HER2 (human epidermal growth factor receptor 2) -positive ($HER2^+$), and triple-negative (TN, $ER^-/PR^-/Her2^-$) BC. Regarding its classification according to molecular features, which is based on mRNA signatures such as PAM50®, BC is categorized into five molecular intrinsic subtypes: Luminal A, Luminal B, HER2-enriched, Basal-like and Normal-like, which partially overlap with the subtypes determined by IHC previously described. The BC IHC subtypes directly condition the clinical approach of patients (Dai et al., 2015).

In this project, we will focus on ER^+ BC, which comprises around 70% of BC cases. Endocrine therapy (ET) is the cornerstone of the treatment for this cancer subtype, which involves treatment with either ERα antagonists (e.g., tamoxifen) or aromatase inhibitors (e.g., letrozole) (Almeida et al., 2021).

ER is essential for normal breast physiology but, in ER^+ tumours, ER acts as a hormone-dependent transcription factor that controls the expression of genes associated with tumour cell survival and proliferation (Wang & Yin, 2015). These patients usually present a positive prognosis, but the major clinical problem of this subtype is that some patients develop resistance to endocrine therapy, and eventually relapse, which significantly affects their survival (Loibl et al., 2021). In fact, up to 20% of patients diagnosed with operable ER^+ tumours recur with metastatic disease within 2–5 years after treatment (Fan et al., 2015).

VAV3 and its role in cancer

Resistance to endocrine therapy is commonly driven by ligand-independent ERα reactivation, which includes a wide range of mechanisms such as mutations in ERα, altered interactions of ERα with coactivators/corepressors, and cross-talk between ERα and growth factor receptors and oncogenic signalling pathways (Ali and Coombes, 2002). In the context of ET resistance, *Aguilar et al., 2014* found that a guanine nucleotide exchange factor (GEF) for small GTP-binding proteins (mainly, for Rho and Rac families), called VAV3, promotes resistance to ETs. The relevance of *in vitro* results was validated in patients by IHC. According to their study, a positive feedback mechanism takes place between VAV3 and ERα, considering that they have a mutual expression crosstalk. In addition, they showed that *VAV3* expression may be more dependent on ERα in the endocrine therapy-resistant setting.

Two major transcript variants of the human *VAV3* gene are generated through alternative splicing: the full-length *VAV3α* and the N-terminally truncated *VAV3.1* (Trenkle et al., 2000). When most of the authors describe VAV3 and its general actions as a GEF, they usually refer to VAV3α, although it is known that VAV3.1 also has oncogenic activity (Boesch et al., 2018). VAV3.1 lacks the catalytic domain and cannot facilitate nucleotide exchange on Rho/Rac GTPases as VAV3α does, and consequently, its oncogenic activity must be the result of other, as-yet-undetermined molecular pathways. Although it has not been totally proven, one possible theory is that VAV3.1 has a regulatory function on the full-length VAV3α by competition (Boesch et al., 2018). VAV3.1 may saturate VAV3α binding sites in its targets, potentially resulting in a dominant negative impact on VAV3α function.

It has been found that *VAV3* is overexpressed and plays a significant role in the tumorigenesis of some cancers such as acute lymphocytic leukaemia (Nayak et al., 2022), colorectal cancer (Uen et al., 2015), pancreatic cancer (Tsuboi et al., 2016) and prostate cancer (Lyons & Burnstein, 2013). Indeed, *VAV3* is upregulated in models of castration-resistant prostate cancer progression and enhances androgen receptor (AR) activity (Lyons & Burnstein, 2013). This mechanism shares some similarities with the one described by *Aguilar et al., 2014* for ET-resistant BC, as VAV3 seems to be cross-regulated with both endocrine receptors, ER and AR. Nevertheless, while the pathways by which prostate cancer cells exploit VAV3 signalling to promote AR activity have been widely described (e.g., Dong et al., 2006; Lyons & Burnstein, 2013; Chen et al., 2015), the characterisation of VAV3 in ET-resistant BC setting is still quite unresolved. Therefore, this project will investigate VAV3 as a novel mediator of ET resistance in ER^+ breast tumours, as well as its role as a relevant prognostic and predictive biomarker and/or a future therapeutic target.

Short hairpin RNA technology

Short hairpin RNAs (shRNAs) are synthetic RNA sequences encoded in DNA vectors that can be introduced into cells via plasmid transfection or viral infection (Moore et al., 2010). Once the vector has been incorporated into the host genome, the shRNA is then transcribed by polymerase II or III depending on its promoter. They spontaneously form hairpin structures that are recognized by RNA interference (RNAi) machinery of the host cell. This way, shRNAs are transformed into siRNAs (small interfering RNAs), which lead to gene silencing either by mRNA cleavage or translation inhibition. The most common way to introduce shRNAs into mammalian cells is by infection with viral particles, allowing their integration into the host genome and causing long-term silencing of the targeted gene. This long-term silencing can be promoted by selecting infected cells with antibiotics (e.g., puromycin) in case the DNA vector carrying the shRNA also encodes a gene driving antibiotic resistance.

Previous experiments in our lab to reproduce data from *Aguilar et al., 2014* had been focused on transfecting human ER^+ BC cell lines with siRNAs targeting *VAV3*. The results obtained had not been as expected, since VAV3 silencing did not show any differential effect between the ET-resistant and the control BC cells. Thereupon, this project is focused on the use of shRNAs targeting *VAV3* in the mammalian cells of interest to investigate its role in the ET resistance setting.

2. HYPOTHESIS AND OBJECTIVES

As previously stated, VAV3 might potentially possess an important oncogenic activity and promote ET resistance in ER^+ breast tumours. Hence, the major objectives of this project are the following: (1) To analyse VAV3 gene and protein expression in BC patients data and *in vitro* models to assess the relationship between VAV3 levels and ER status in BC; (2) To examine if endocrine therapy-resistant cells present significantly higher VAV3 levels in comparison to control ER^+ cells; (3) To generate lentiviral particles carrying different shRNAs designed to target *VAV3*, which will be used in the future to evaluate the effect of *VAV3* silencing in the context of ET resistance.

3. MATERIALS AND METHODS

Cell cultures

MCF-7 cells (HTB-22™, ATCC) were selected as a well-established model of ER^+ BC. MCF-7-derived LTED (abbreviated as LTED, long-term oestrogen deprivation) cells are considered a model of acquired resistance to endocrine therapies (Maximov et al., 2022). LTED cells were generated in the group, previous to my incorporation, from MFC-7 cells by removal of oestrogens in the culture medium, which initially slowed their growth and promoted cell death, but, eventually, certain cell clones became resistant to oestrogen absence and repopulated the culture. MCF-7 and LTED cells were cultured in RPMI medium supplemented with 10% FBS, 1% penicillin and streptomycin, and 1% L-glutamine. In the case of LTED cells, in the absence of oestrogens (by using phenol red-free RPMI medium and trypsin, and 10% dextran-coated, charcoal-stripped serum (Welshonst & Jordan, 1987).

To generate lentiviral particles, HEK293T cells (ATCC, embryonic cells isolated from human kidney and transfected with T antigen) were cultured in complete Dulbecco's Modified Eagle's Medium (DMEM), containing 10% FBS, 1% penicillin and streptomycin, and 1% L-glutamine (all of them from Gibco® Life Technologies).

Cells were maintained in a humidified atmosphere at 37ºC and 5% CO_2, and trypsinized and subcultured before confluency reached 70-80% following standard protocols. Moreover, mycoplasma analyses were monthly performed by PCR (Polymerase Chain Reaction) and morphology was daily checked by microscopy.

Gene expression analysis

RNA extraction and retrotranscription

RNA was extracted from cell pellets of a panel formed by 21 different human BC cell lines as well as a non-tumour human mammary epithelial cell line (MCF10A) (Supplementary Table 1). Extra cell pellets from MCF-7 and LTED cells were also collected. In all of them, Trizol was used for cell lysis and chloroform for RNA extraction, followed by RNA precipitation with isopropanol, according to standard protocols. Concentration and purity (A_{260}/A_{280} ratio) of the RNA in the samples were measured with the Spectrophotometer (Thermo Scientific NanoDrop 1000), using ND software (Nucleic Acid, RNA). Afterwards, 1µg of total RNA was retrotranscribed to complementary DNA (cDNA) using Maxima First Strand cDNA Synthesis kit, following the manufacturer's instructions. The obtained product was diluted to 0.5 ng/µl.

qRT-PCR (Quantitative Real-Time Polymerase Chain Reaction)

A total of 10 µl volume was added to each well in a 384-well plate, containing 4 µl of cDNA (stock at 0.5 ng/µl), 1 µl of forward and reverse primers (stocks at 1 µM, sequences available in Supplementary Table 2) and 5 µl of Power SYBER® Green PCR Master Mix (Applied Biosystems). Two housekeeping genes, *HPRT* and *ACTB,* were used for normalisation (Supplementary Table 2). Triplicates of each condition were done. For the negative control, distilled water was used instead of cDNA.

Once the plate was prepared, it was placed in the BioRad CFX384 Real-Time PCR System from the Genomic Facility of IIS Biodonostia with the following PCR programme: (1) Preincubation: 2 minutes at 50°C and 10 minutes at 95°C; (2) Amplification: 45 cycles of 15 seconds at 95°C and 1 min at 60°C; (3) Melting curve: 10 seconds at 95°C, 1 minute at 65°C and one second at 97°C. Expression values were calculated following the method of *Pfaffl, 2001*.

Protein levels analysis by Western blot

Protein extraction and quantification

Proteins were extracted from pellets of a panel formed by 21 different human BC cell lines (Supplementary Table 1). Cells were lysed in RIPA lysis buffer (Supplementary Table 3) and cell lysis was favoured by vortexing. Centrifugation was carried out at 12.000 x g for 10 minutes (at 4ºC) and supernatants containing cell proteins were carefully transferred to new tubes. Total protein concentration was determined by BCA assay (Pierce BCA Protein Assay Kit, Thermo Fisher Scientific), measured by the Spectrophotometer (Thermo Scientific 1000). The absorbance values were extrapolated to a curve of known concentrations of BSA (bovine serum albumin) (0.25; 0.5; 1; 1.5 and 2 µg/µl) to calculate the protein concentration of each sample.

Electrophoresis and Western Blot

For each sample, 20 µg of total protein were prepared in protein loading buffer (Supplementary Table 3). After 10 min of sample heat shock at 95ºC (to denature proteins) and spinning, 15 µl of each sample were loaded onto commercial 8-12% acrylamide gels (mini-PROTEAN® TGX™ gels, BIO-RAD). In turn, 8 µl of Precision Plus Protein™ Kaleidoscope™ marker (BIO-RAD) were loaded into the first well of each gel. Proteins were run in an electrophoretic buffer (Supplementary Table 3) at 110 V for approximately 1 hour.

After the electrophoresis, transfer of the proteins to nitrocellulose membranes (Trans-Blot Turbo Transfer Pack, BioRad, #1704158) was carried out using Bio-Rad "MIXED MW" programme in a Transfer-Blot Turbo system (Bio-Rad). Then, membranes were stained with Ponceau S (Life Science, Sigma Aldrich, (#6226-79-5) to ensure that proteins were correctly transferred to the nitrocellulose membranes.

Membranes were blocked with 5% skimmed-milk in TBST buffer (Supplementary Table 3) for 1 hour prior to incubation with each primary antibody. Primary antibody (anti-VAV3, Millipore, #07-464; or anti-β-actin, Sigma-Aldrich, #5441) was diluted at 1:1000 in 5% skimmed-milk TBST and incubated at 4ºC overnight. The next day, 3 washings with TBST were performed. Secondary antibody (anti-rabbit, GE Healthcare, #Na931v; or anti-mouse, Merck-Sigma, #GENA934) was diluted at 1:2000 in 5% skimmed milk TBST and incubated for 1 hour at room temperature. Before chemoluminescence detection, 3 washings with TBST were performed. For protein detection, membranes were incubated for 2 minutes with Novex™ ECL Chemiluminescent Substrate Reagent Kit (Solution A + Solution B in a 1:1 ratio, Thermo Fisher, #WP20005).

As secondary antibodies were coupled to horseradish peroxidase enzyme (HRP) and ECL contains its substrate (luminol), chemiluminescence was produced and the signal was captured by an iBrightTM CL750 Imaging System (Thermo Fisher). To reincubate membranes with different primary antibodies, membranes were stripped using a Restore™ Western Blot Stripping Buffer (Thermo Fisher) for 20 minutes in the shaker.

ImageJ image analysis programme was employed for signal quantification of the bands of interest in the membranes, using β-actin to normalize the levels of protein detected.

Analysis of patients' public databases

Cancertool (Cortazar et al., 2018) and Kaplan-Meier Plotter (Lánczky & Győrffy, 2021) bioinformatics tools were used to perform various analyses of patients' data. These webtools integrate data from different publicly available studies, in this case, from various clinical BC studies. Gene expression of breast tumour samples and patients' associated clinical data (e.g., RFS, recurrence-free survival) were obtained from and represented by this software.

Generation of lentiviral particles containing shVAV3 plasmids

Plasmids amplification, purification and verification

We used commercial pLKO.1 vectors, each one containing a different insert designed to target either VAV3α, VAV3.1 or both isoforms when introduced into mammalian host cells by shRNA technology (denoted as shVAV3 plasmids). In addition, a vector with no target gene (scramble shRNA) was used as the negative control. Further details about them can be found in Supplementary Table 4 and Supplementary Figure 1.

In order to amplify plasmids, bacterial transformations were performed using One Shot™ TOP10 chemically competent *E. coli* cells (Invitrogen™, #C404003) by heat shock and according to the manufacturer's standard protocol. Negative control was acquired by applying 1 µl of distilled water as a replacement for plasmids. Transformed bacteria were spread on LB agar plates containing ampicillin (100 µg/ml, Sigma Aldrich, #A9518), since procaryotic ampicillin resistance sequences were included in pLKO.1 vectors (Supplementary Figure 1).

After incubating the plates at 37ºC overnight, colonies were picked and re-grown in 5 ml liquid LB medium containing ampicillin (100 µg/ml) and, in some cases, chloramphenicol (CAP; 0, 3, 5, 10 and 25 µg/ml) at 37ºC or 30ºC for 6-8h (CAP treatment and incubation at 30ºC were used to optimize the protocol, as it will be explained in detail in section '4. RESULTS, plasmid purification'). When indicated, bacterial growth was prolonged for 24 hours to increase plasmid amplification.

Bacterial growth was measured using the spectrophotometer at 680 nm (optical density, OD) and LB medium as blank. Plasmid purification was carried out using QIAprep Spin Miniprep Kit (QIAGEN) and according to the manufacturer's protocol. The final concentration of plasmid DNA was measured by the Spectrophotometer (Thermo Scientific NanoDrop 1000) using ND software (Nucleic Acid, DNA).

We also confirmed by restriction enzyme analysis that we had purified pLKO.1 vectors. For that, we used BsaI restriction enzyme (Biolabs, #R0535S; Supplementary Figure 1) for DNA digestion and compared the resulting DNA fragments separated in agarose gels with those predicted by Benchling bioinformatics tool. Taking into account that 10 units of restriction enzyme are sufficient for digestion of 1 µg of plasmid (amount used), 1 µl of BsaI enzyme was employed (stock: 10.000 U/ml), and the DNA cleavage was achieved by

incubating the mixture overnight at 37 ºC. For each plasmid, negative controls of the digestion were prepared by adding 1 µl of distilled water rather than the restriction enzyme. Then, digestion products were run in 1% agarose gels (manually prepared by boiling 0.5 g of agarose in 50 ml of TBE buffer (Supplementary Table 3), adding 5 µl of GelRed for subsequent DNA detection, and letting the gel polymerize). DNA Loading Dye (Thermo Fisher Scientific, #R1161; Supplementary Table 3) was added to each sample and the gel was loaded with 5 µl of marker (Thermo Fisher Scientific, #SM0242) and 15 µl of each sample. DNA fragments were run in TBE buffer at 110V for approximately 1 hour. Invitrogen™ iBright™ CL750 Imaging System (Thermo Fisher) was used to detect the fluorescent signal produced by GelRed when interacting with dsDNA (double-stranded DNA).

Lentiviral particle production: HEK293T transfection & particle recollection

HEK293T cells were used for the production of lentiviruses. For that purpose, HEK293T cells were transfected with each plasmid of interest along with plasmids containing sequences that encode essential genes for lentiviral particle generation (*RRE*, *REV* and *VSV*). 24 hours before this transfection, cells were seeded at a density that guaranteed 50-60% confluence the next day in p100 plates (each plasmid required 1 plate). To increase the viral production rate, plates were coated with sterile gelatin (2% in water) for 20 minutes and washed with PBS (phosphate-buffered saline) before seeding. To perform the transfection, transfection cocktails were prepared with the following reagents: 960 µl of Optimem medium, 9.2 µl Turbofect (Thermo Fisher Scientific), 2.57 µg pMDLg-pRRE, 1 µg pRSV-REV, 1.42 µg pMD2.G (the three plasmids encoding the lentiviral packaging components) and 5 µg plasmid of interest (5 different shVAV3 and scramble, Supplementary Table 4). An additional cocktail containing distilled water instead of the three lentiviral packaging components and the plasmid of interest was prepared as a negative control. After 20 minutes of incubation at room temperature, cocktails were added drop-wise to HEK293T cells cultured in antibiotic-free DMEM medium. 6 hours after transfection, the medium was replaced by 7 ml of complete DMEM medium, and, after 72 hours, HEK293T supernatant containing the lentiviral particles was centrifuged at 800 rpm for 5 minutes and filtered with 0.45 µm filters.

Viral titration

HEK293T cells were seeded in 6 multiwell plates (1 plate per supernatant to test) at 30% confluence in complete DMEM medium. After 24 hours, cells were infected with increasing volumes (from 0 µl to 500 µl) of supernatants containing lentiviral particles (previously obtained) and polybrene (10 µg/ml, Sigma Aldrich, #S2667). Next day, the medium was replaced by a fresh one and, after 48 hours, cells were selected with puromycin (1µg/ml, Thermo Fisher Scientific, #A1113803). After 7 days, cells were fixed and stained with violet crystal (0.2%) (Sigma Aldrich, #C-0775)- ethanol (2%) solution. Antibiotic-resistant coloured colonies were counted and the number of viral particles/ml of supernatant was estimated.

Statistical analyses

For statistical analyses, GraphPad Prism 8.0.1 software was used. A 95% confidence interval was applied for all tests (significant values below $\alpha = 0.05$). Unpaired and paired t-tests were used depending on the nature of the data to analyse. Error bars denote the standard error of the mean (SEM). * indicates p-value < 0’05; ** p < 0’01 and ***, p < 0’001. ‘ns’ means that the difference between groups is ‘not significant’.

4. RESULTS

VAV3 mRNA levels are higher in ER$^+$ cell lines

To start with, *VAV3* mRNA levels were analysed by qRT-PCR in a panel of 21 BC cell lines (Figure 1). MCF-7 cell line (sample #15) was used as the reference to represent *VAV3* mRNA levels due to its importance as an ER$^+$ BC *in vitro* model. *HPRT* and *ACTB* were used as housekeeping genes for *VAV3* gene expression normalisation. As shown, total *VAV3*, *VAV3α* and *VAV3.1* expressions were separately examined. The most notable peaks in the three graphs mainly belonged to ER$^+$ cell lines such as T47D (sample #14) and BT-474 (sample #17). MCF10A cells (a non-tumour human mammary epithelial cell line) showed very low *VAV3* gene expression (sample #18). Of note, MDA-MB-453 cells (sample #21), an *in vitro* model of ER$^-$ that is considered luminal by gene expression, presented high expression of *VAV3α*.

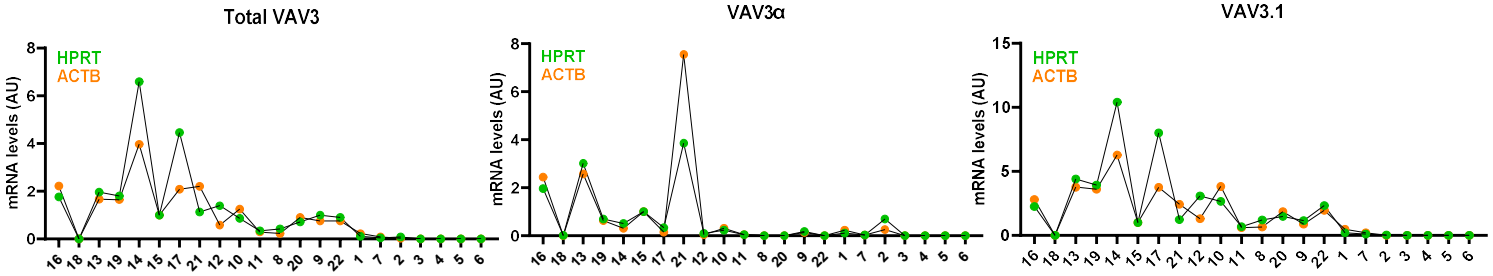

Figure 1. qRT-PCR results of total *VAV3*, *VAV3α* and *VAV3.1* mRNA levels in a panel of BC cell lines. Reference sample: MCF-7 cells (#15). Values are normalised using *HPRT* and *ACTB* housekeeping genes. Cell lines are denoted with numbers specified in Supplementary Table 1.

Indeed, when dividing cell lines from the BC panel by their ER status, it was more easily observed that total *VAV3* and both *VAV3α* and *VAV3.1* isoforms gene expression levels were significantly higher in ER$^+$ than in ER$^-$ cell lines (Figure 2).

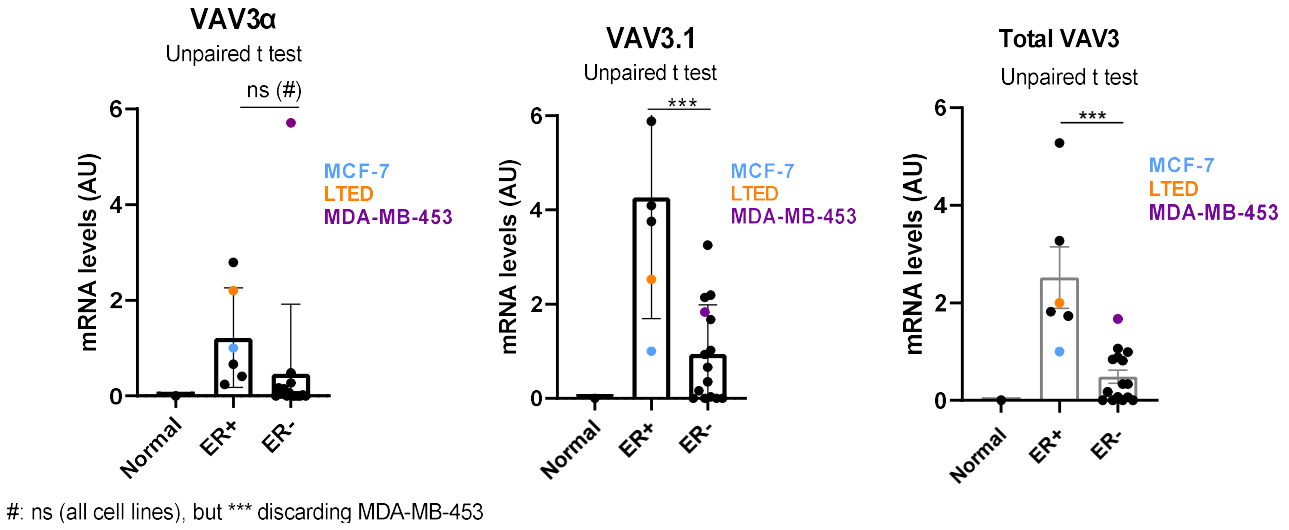

Figure 2. qRT-PCR results of total *VAV3*, *VAV3α* and *VAV3.1* expression levels in a panel of BC cell lines classified by ER status. Different colours are used to highlight specific cell lines of interest. 'AU' refers to arbitrary units.

There is no statistically significant difference in *VAV3* gene expression between MCF-7 and LTED cells

A specific aim of this project was based on deciphering whether VAV3 is implicated in resistance to ET in ER$^+$ BC patients. For that purpose, as previously mentioned, we used a cell model that reproduces ET

resistance. We examined if there were *VAV3* expression differences between MCF-7 (sensitive to oestrogen deprivation) and LTED (MCF-7 derivates, resistant to oestrogen deprivation) cells.

Paired t-tests of qRT-PCR results (with four biological replicates) demonstrated that, even though there might be a trend of increased expression in some isoforms and some samples from LTED cells compared to MCF-7, differences were not consistent or statistically significant.

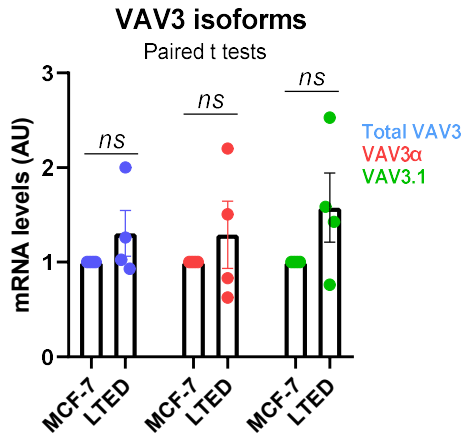

Figure 3. qRT-PCR results of total *VAV3*, *VAV3α* and *VAV3.1* mRNA levels in MCF-7 and LTED cell lines. N=4.

In patients' data, *VAV3* gene is overexpressed in ER⁺ BC tumours compared to ER⁻

To increase the translational potential of our project, we not only examined *VAV3* mRNA levels *in vitro*, but also in BC patients' *in vivo* data from Cancertool (Cortazar et al., 2018) and Kaplan-Meier plotter (Lánczky & Győrffy, 2021) databases (Figure 4). Concerning *VAV3* gene expression in BC patients divided by ER status, *in vivo* results correlated with our previous *in vitro* outcome, as ER⁺ BC patients revealed higher *VAV3* expression (Figure 4a). In addition, *VAV3* levels seemed to have a significant effect on recurrence-free survival (RFS) when considering all BC subtypes, whereas when selecting the ER⁺ patients who had received ET, our particular setting of interest, VAV3 levels did not have an impact on RFS (Figure 4b).

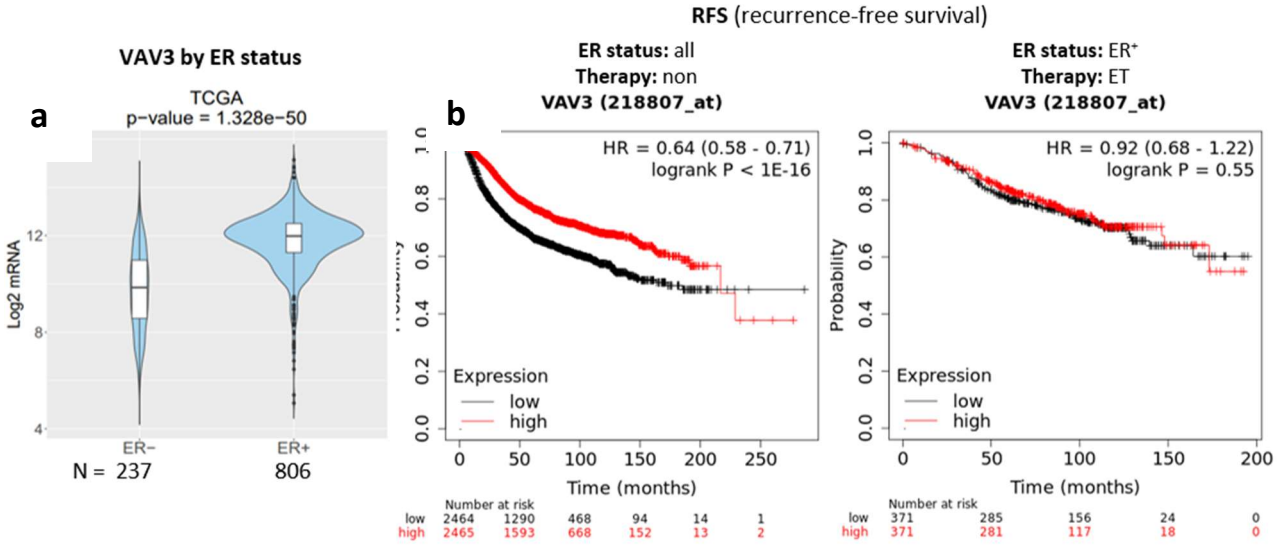

Figure 4. Patients' data from BC patients. **a**) *VAV3* mRNA levels of patients' breast cancer samples classified by ER status. Webtool: Cancertool (Cortazar et al., 2018). **b**) Recurrence-free survival (RFS) of BC patients of all subtypes without treatment filtering (left) and ER⁺ patients who received ET (right) according to VAV3 expression (high vs low) in their tumour samples. Webtool: Kaplan-Meier Plotter (Lánczky & Győrffy, 2021).

Preliminary analysis indicates that ER status does not condition VAV3 protein levels

Next, we decided to check whether VAV3 protein levels correlated with gene expression data. Western Blot results are presented in Figure 5. Of note, β-actin signal was not homogeneous in every sample, although it was directly proportional to the one obtained by Ponceau S staining, indicating that quantification must be considered preliminary. Moreover, multiple bands were detected by the antibody. Among others, bands at the expected molecular weight of VAV3α (87 kDa) and VAV3.1 (33 kDa) isoforms could be observed in the membranes. However, there were no clear differences in terms of VAV3 levels in different BC subtypes or segregation according to ER status. Although VAV3α protein levels were slightly higher in ER^+ cells, the result was not statistically significant. In the case of VAV3.1, levels did not differ between ER^+ and ER^- cell lines. In general, Western Blot quality needs to be optimised and its interpretation needs further investigation.

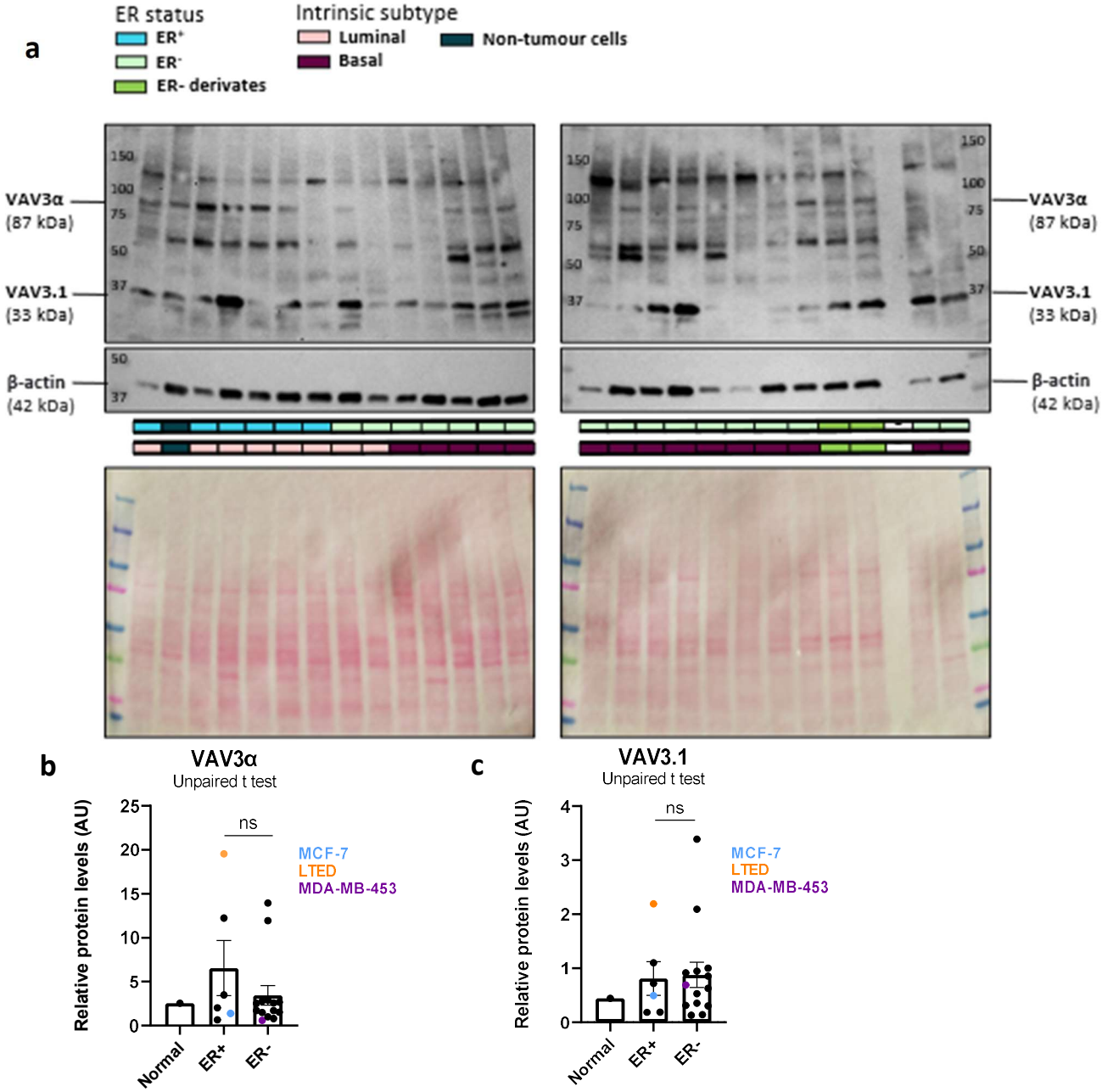

Figure 5. VAV3 protein levels in BC panel cell lines analysed by Western Blot. **a**) Full membrane of Western blot using anti-VAV3 antibody, indicating VAV3α and VAV3.1 molecular weights, with a housekeeping Western Blot using anti-β-actin antibody (used for normalisation). Fold change of VAV3α (**b**) and VAV3.1 (**c**) in BC panel cell lines relative to HCC1954 cells (repeated sample in the gels). Colours are used to highlight specific cell lines of interest.

Lentiviral particles carrying shRNAs to silence *VAV3* expression were properly generated

Optimisation of pLKO.1 plasmids amplification

Once the importance of VAV3 in ER$^+$ BC *in vitro* models and patients' data were examined, we developed tools for VAV3 silencing in those cells.

As represented in Figure 6, plenty of bacterial colonies were obtained after the transformation with the pLKO.1 plasmids previously mentioned (Supplementary Table 4). Under the effect of ampicillin in the agar plates, bacterial cells that lack a plasmid with the ampicillin resistance gene were unable to survive. Therefore, no colonies could be observed in the NC (negative control) petri plate.

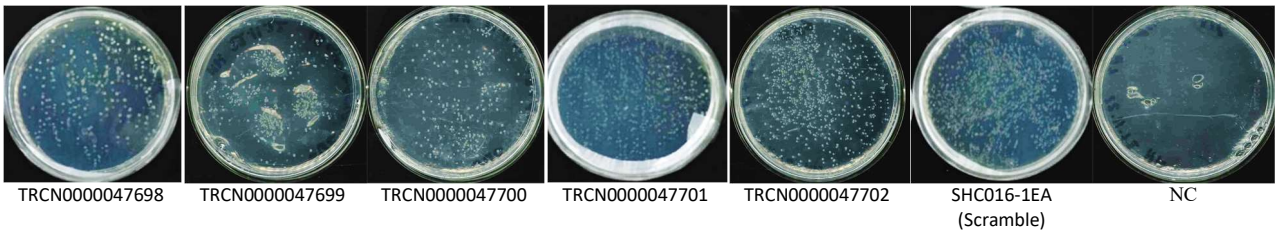

Figure 6. Petri plates with bacterial colonies obtained in the presence of ampicillin after transformation of One Shot™ TOP10 chemically competent *E. coli* cells with pLKO.1 vectors each one with a different shRNA insert targeting VAV3.

As we obtained low plasmid amounts with a standard protocol for plasmid amplification, we opted to search for specific protocols for the optimisation of plasmid amplification conditions (Wegrzyn & Wegrzyn, 2002; Begbie et al., 2005), which led us to decrease incubation temperature (from 37ºC to 30ºC) and use CAP at low doses to increase the efficiency of plasmid amplification. On the one hand, the total plasmid amount obtained after several bacterial incubations at different temperatures and CAP concentrations is represented in Figure 7a. On the other hand, plasmid:bacteria ratio was calculated and shown in Figure 7b, which gives an idea of the amount of plasmid present in each bacterial unit.

Effectively, the total amount of plasmid increased by incubating bacteria at 30ºC (Figure 7a). While we observed a decrease in the total amount of plasmid caused by CAP (Figure 7a), the plasmid:bacteria ratio was similar to that at 30ºC without CAP (Figure 7b). Therefore, CAP usage could still show promising results if bacteria were cultivated for longer. 5 µg/ml was arbitrarily chosen for longer incubation (24 hours) together with the condition lacking CAP. Regarding the condition of 5 µg/ml of CAP, it was clear that 24 hours of extra incubation resulted in a notable increase of total plasmid, but, since bacteria did not show high growth, the total amount of plasmid was still insufficient. On the contrary, we could observe that in the bacterial suspension without CAP an adequate amount of plasmid was obtained (Figure 7a), sufficient for oncoming HEK293T cells transfection.

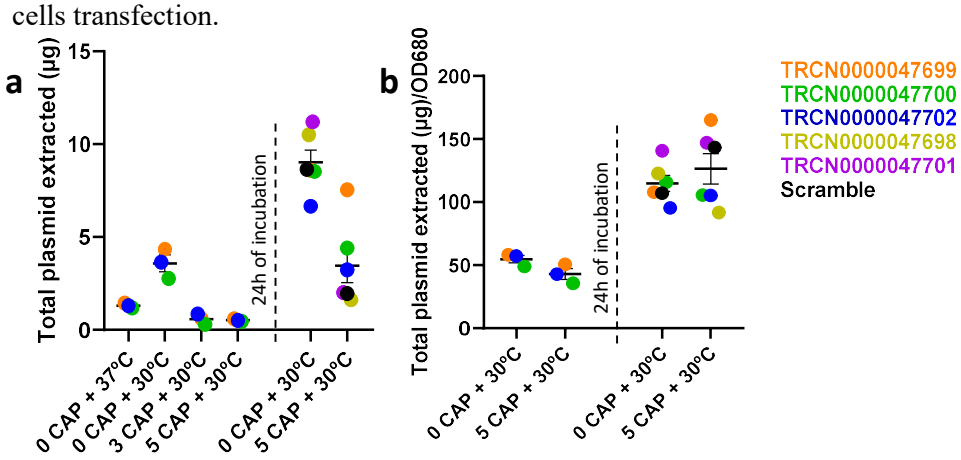

Figure 7. (**a**) Total plasmid extracted (µg) and (**b**) plasmid:bacteria ratio (µg/OD680) obtained by variating incubation conditions, i.e., temperature and CAP concentration, in each bacterial suspension transformed with a specific plasmid (Supplementary Table 4).

BsaI restriction enzyme assay confirms *in silico* digestion of pLKO.1 plasmids

Once we had an adequate amount of plasmid, we analysed whether the plasmids were pLKO.1 as they should be. We performed a BsaI restriction enzyme assay and compared it with an *in silico* digestion (Figure 8a). The iBright images attained from the agarose gel electrophoresis (Figure 8b) showed positive results. Plasmid DNA was cleaved by BsaI restriction enzyme as expected, since five different fragments were generated from each plasmid, matching the theoretical sizes shown in Figure 8a. Moreover, negative controls (NC) displayed bands belonging to non-digested plasmids, which could correspond to supercoiled and nicked plasmids in the upper bands and circular plasmid molecules in the lower band.

Even though this experiment did not allow us to confirm our pLKO.1 vectors had the correct insert, the presence of the appropriate vector was verified, giving us the reliance to continue with the protocol and to use the purified plasmids for HEK293T cells transfection and lentiviral particle generation.

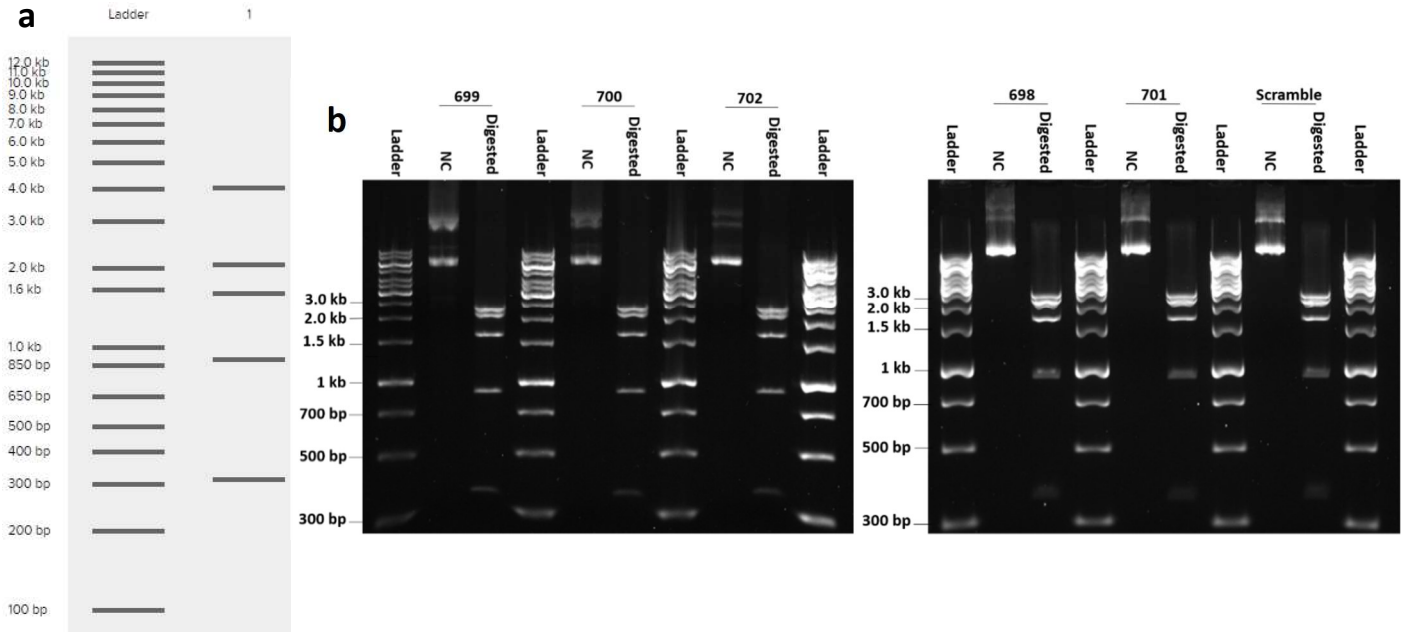

Figure 8. *In silico* (**a**) and obtained (**b**) enzymatic digestion of all our pLKO.1 vectors (scramble and each one with a different shVAV3 insert). 'NC' means negative control, where no restriction enzyme was added. Plasmid names in the graph are given according to the last three numbers of their code (for plasmid description, view Supplementary Table 4).

Functional lentiviral particles were generated, ready to silence *VAV3* expression in MCF-7 and LTED cells

After transfecting HEK293T cells with each shRNA plasmid of interest and plasmids containing sequences encoding essential genes for lentiviral particles production, their supernatants were used to infect HEK293T cells and conduct a viral titration. Figure 9 shows an example of a 6 multiwell plate containing infected HEK293T cells selected with puromycin and stained with violet crystal (plasmid # TRCN0000047699). The larger the volume of supernatant with lentiviral particles used, the higher the number of survivor colonies. By counting puromycin-resistant coloured colonies, the number of viral particles/ml of supernatant was calculated (Table 1). In this case, wells belonging to 10 and 50 µl of supernatant with lentiviral particles were used for quantification. Of note, we did not detect colonies nor in the condition without supernatant added (0 ul) neither in the plate treated with the supernatant from untransfected HEK293T cells (data not shown).

Table 1. Number of viral particles/ml of supernatant in each sample containing a specific plasmid.

Commercial clone ID (Sigma-Aldrich)	Number of viral particles/ml of supernatant ± SEM
TRCN0000047700	185 ± 3
TRCN0000047698	750 ± 21
TRCN0000047702	1400 ± 141
TRCN0000047699	1310 ± 53
TRCN0000047701	1800 ± 35
Scramble	200 ± 9

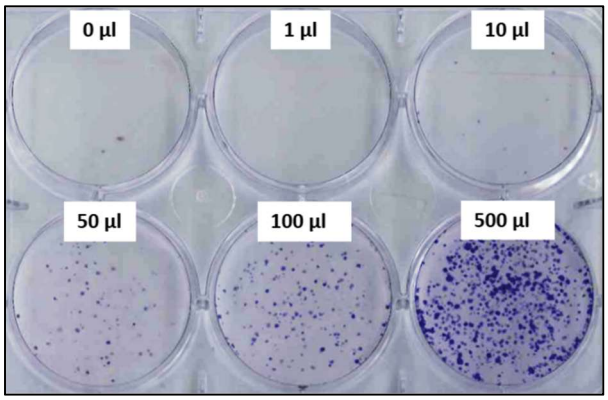

Figure 8. 6 multiwell plate containing HEK293T cells infected by an increasing volume (0, 1, 10, 50, 100, 500 µl) of supernatant with lentiviral particles. Colonies were coloured with crystal violet to improve their visualisation and quantification.

5. DISCUSSION

Over the past few decades, endocrine therapy has significantly increased the survival rates of ER^+ BC patients; nonetheless, resistance to this treatment continues to be one of the leading causes of BC death today (Matsumoto et al., 2015). For this reason, there is no doubt that the identification of resistance mechanisms is paramount, in an effort to find strategies to counteract the resistance and develop new therapies.

Inside the broad field of ET resistance mechanisms, the role of VAV3 has drawn the attention of scientists working in human BC, as well-described by *Lee et al., 2008* and *Aguilar et al., 2014*, being the latter the main study our lab focused on. Research made by (Aguilar et al., 2014) included the use of three different shRNA sequences targeting VAV3 on the one hand, and one for ERα, on the other hand. As ERα depletion led to a notable VAV3 protein level decrease in ET-resistant cells, they were successful in proving the strong dependence of VAV3 on ERα in the resistance setting. In addition, VAV3 silencing resulted in a significant proliferation decline in LTED cells, which supported the idea of VAV3 playing an important role in resistance.

In this context, our main approach was based on conducting a deep analysis of the role of VAV3 in resistance to ET. For that purpose, we tried to recapitulate the shRNA-mediated VAV3 depletion experiment performed by *Aguilar et al., 2014*, bearing in mind that LTED cells could vary from one research group to another. Importantly, previous examinations using anti-VAV3 siRNAs generated confusing results which also led us to repeat and refine this project (before my incorporation, data not shown).

Before moving to the *in vitro* models, we aimed to determine if VAV3 (at transcriptomic or protein level) is increased in ER^+ tumours compared to ER^-, as well as to examine an assumption that was not proved by *Aguilar et al., 2014*: whether *VAV3* gene expression is increased in ET-resistant cells when compared to MCF-7 BC cells. As presented in Figures 1 and 2, ER^+ BC cell lines showed a significantly higher amount of *VAV3* mRNA levels compared to ER^- cells, with *p* values lower than 0.05. Since this was also confirmed *in vivo* by Cancertool (Cortazar et al., 2018) data analysis (Figure 4a), VAV3 may be an important molecule for ER^+ tumour survival and progression. What is more, a specific study in a cohort of ER^+ BC patients found mutations in *VAV3*, supporting the correlation between the impact of VAV3 and ER positivity (Schwartz et al., 2021).

However, it needs to be taken into consideration that not all scientific studies relate VAV3 with ER positivity. For instance, *Chen et al., 2015* indicated that according to their experiments, VAV3 protein levels

were significantly higher in ER^- tumours. Indeed, our Western Blot results did not show any association between VAV3 protein levels and ER positivity, which suggests that the transcript of *VAV3* and the protein could have a distinct regulation. The fact that *VAV3* gene expression and protein levels do not correlate could have a clinical impact, considering that pathological analyses of patients' samples are usually carried out by IHC, which measures proteins. Moreover, the finding of more bands than expected in anti-VAV3 Western Blot was of huge importance for us to consider further research regarding the characterisation of signals with an unknown origin or the need to find a more specific antibody.

Concerning the comparison of *VAV3* mRNA levels between LTED and MCF-7 cells (Figure 3), there was no statistical evidence to prove LTED cells had higher *VAV3* expression levels. Clinical data showed similar results, as *VAV3* expression levels in patients did not appear to predict survival in ER^+ patients treated with ET (Figure 4b, right). The reason why a significant difference is obtained when considering all BC patients regardless of their ER status and treatment (Figure 4b, left) is that ER^+ patients are the ones with the highest *VAV3* expression and they usually have higher survival rates.

Regarding our results on plasmid amplification, it is of relevance to mention the main reason why we first failed to obtain enough amount of plasmid after bacterial growth and, consequently, optimisation of bacterial growth conditions was carried out. Plasmids containing a shRNA sequence can cause cytotoxicity to bacterial cells due to their off-target effect (Goel & Ploski, 2022). As a result, our bacteria proliferated with very few plasmid copies, leading to a low plasmid yield. To overcome this issue, on the one hand, we changed the incubation temperature from 37ºC to 30ºC. Actually, plasmid copy number appears to increase at lower temperatures (Wegrzyn & Wegrzyn, 2002). Thanks to this adjustment, plasmid yield was strikingly enhanced, taking as an example the rise from 1.45 µg to 8.6 µg of the plasmid with code #TRCN0000047699. It could be interpreted that the temperature modification worked splendidly in our bacterial suspensions, to the extent that it happened to be adequate for obtaining a sufficient amount of plasmid for HEK293T cells transfection. On the other hand, we tested low doses of CAP (no cytotoxic), an antibiotic that acts upon protein synthesis by inhibiting translation, and, consequently, genomic DNA replication is interrupted while plasmids can still continue to replicate (Begbie et al., 2005). With 5 µg/ul of CAP, slightly higher (or similar) plasmid:bacteria ratios were acquired in comparison to bacterial suspensions lacking CAP. However, our main approach was based on obtaining the highest amount of plasmid possible in order to continue with our protocol by transfecting HEK293T cells, which is why 0 µg/ul CAP concentration was chosen.

By using Benchling bioinformatics programme for finding a suitable restriction enzyme for our plasmids' digestion, no enzyme was found that could differently recognise the inserted sequences. Thus, we chose BsaI, a reasonable enzyme candidate that made specific cleavages in pLKO.1 vector and was already available in our laboratory stock. By performing agarose gel electrophoresis, the band pattern obtained in Figure 8 confirmed that we had purified the correct vectors. As a future step, we do not rule out performing Sanger sequencing of the plasmids, specifically of the inserts, to be absolutely sure that the plasmids are the correct ones.

Finally, the puromycin-resistant HEK293T cell colonies observed in the viral titration were the key to confirm that we succeeded in creating infectious lentiviral particles. Taking into account that VAV3 seems to

contribute to ET resistance in ER^+ BC in conformity with *Aguilar et al., 2014*, our next challenge consists in silencing VAV3 in MCF-7 and LTED cells and conducting a proliferation and tumorigenic assays to assess if VAV3 plays a critical role in acquired resistance.

6. CONCLUSIONS

In summary, this project has identified that *VAV3* gene expression is increased in ER^+ BC *in vitro* and in patients compared to ER^-, whereas we have not obtained significant differences regarding VAV3 protein levels in different BC subtypes. Nonetheless, we could not observe any evidence of an increment of this GEF in the ET-resistant LTED cells. Moreover, we have optimized the amplification (at 30ºC, in the absence of CAP) and characterisation (with BsaI restriction enzyme) of plasmids containing shRNAs sequences (targeting *VAV3* expression and scramble), which have been perfectly integrated into lentiviral particles with infective capacity.

In the near future, lentiviral particles containing shRNAs will be used to infect mammalian MCF-7 and LTED cells for *VAV3* silencing. Analysis regarding cell proliferation will be performed to contrast our outcome with already published data. Furthermore, more research is unquestionably necessary for a better understanding of VAV3α and VAV3.1 isoforms and their underlying processes in resistance to BC ET. In summary, this study contributes to the investigation of VAV3 as a biomarker and/or a future therapeutic target to combat ET resistance in ER^+ BC patients.

7. BIBLIOGRAPHY

Aguilar, H., Urruticoechea, A., Halonen, P., Kiyotani, K., Mushiroda, T., Barril, X., Serra-Musach, J., Islam, A., Caizzi, L., Di Croce, L., Nevedomskaya, E., Zwart, W., Bostner, J., Karlsson, E., Pérez Tenorio, G., Fornander, T., Sgroi, D. C., Garcia-Mata, R., Jansen, M. P. H. M., … Pujana, M. A. (2014). VAV3 mediates resistance to breast cancer endocrine therapy. *Breast Cancer Research*, *16*(3). https://doi.org/10.1186/bcr3664

Almeida, C. F., Teixeira, N., Oliveira, A., Augusto, T. V., Correia-da-Silva, G., Ramos, M. J., Fernandes, P. A., & Amaral, C. (2021). Discovery of a multi-target compound for estrogen receptor-positive (ER+) breast cancer: Involvement of aromatase and ERs. *Biochimie*, *181*, 65–76. https://doi.org/10.1016/J.BIOCHI.2020.11.023

Begbie, S., Dominelli, G., Duthie, K., Holland, J., & Jitratkosol, M. (2005). The Effects of Sub-Inhibitory Levels of Chloramphenicol on pBR322 Plasmid Copy Number in Escherichia coli DH5α Cells. In *Journal of Experimental Microbiology and Immunology (JEMI)* (Vol. 7).

Boesch, M., Reimer, D., Sopper, S., Wolf, D., & Zeimet, A. G. (2018). (Iso-)form Matters: Differential Implication of Vav3 Variants in Ovarian Cancer. *The Oncologist*, *23*(7), 757–759. https://doi.org/10.1634/theoncologist.2017-0683

Chen, X., Chen, S., Liu, X. A., Zhou, W. Bin, Ma, R. R., & Chen, L. (2015). Vav3 oncogene is upregulated and a poor prognostic factor in breast cancer patients. *Oncology Letters*, *9*(5), 2143–2148. https://doi.org/10.3892/ol.2015.3004

Cortazar, A. R., Torrano, V., Martín-Martín, N., Caro-Maldonado, A., Camacho, L., Hermanova, I., Guruceaga, E., Lorenzo-Martín, L. F., Caloto, R., Gomis, R. R., Apaolaza, I., Quesada, V., Trka, J., Gomez-Muñoz, A., Vincent, S., Bustelo, X. R., Planes, F. J., Aransay, A. M., & Carracedo, A. (2018). Cancertool: A visualization and representation interface to exploit cancer datasets. *Cancer Research*, *78*(21), 6320–6328. https://doi.org/10.1158/0008-5472.CAN-18-1669/653397/AM/CANCERTOOL-A-VISUALIZATION-AND-REPRESENTATION

Dai, X., Li, T., Bai, Z., Yang, Y., Liu, X., Zhan, J., & Shi, B. (2015). Breast cancer intrinsic subtype classification, clinical use and future trends. *Am J Cancer Res*, *5*(10), 2929–2943. www.ajcr.us/

Dong, Z., Liu, Y., Lu, S., Wang, A., Lee, K., Wang, L. H., & Revelo, M. (2006). Vav3 oncogene is overexpressed and regulates cell growth and androgen receptor activity in human prostate cancer. *Molecular Endocrinology*, *20*(10), 2315–2325. https://doi.org/10.1210/me.2006-0048

Fan, W., Chang, J., & Fu, P. (2015). Endocrine therapy resistance in breast cancer: current status, possible mechanisms and overcoming strategies. *Future Medicinal Chemistry*, *7*(12), 1511. https://doi.org/10.4155/FMC.15.93

Goel, K., & Ploski, J. E. (2022). RISC-y Business: Limitations of Short Hairpin RNA-Mediated Gene Silencing in the Brain

and a Discussion of CRISPR/Cas-Based Alternatives. *Frontiers in Molecular Neuroscience*, *15*, 346. https://doi.org/10.3389/FNMOL.2022.914430/BIBTEX

Harbeck, N., Penault-Llorca, F., Cortes, J., Gnant, M., Houssami, N., Poortmans, P., Ruddy, K., Tsang, J., & Cardoso, F. (2019). Breast cancer. *Nature Reviews Disease Primers*, *5*(1). https://doi.org/10.1038/s41572-019-0111-2

Lánczky, A., & Győrffy, B. (2021). Web-based survival analysis tool tailored for medical research (KMplot): Development and implementation. *Journal of Medical Internet Research*, *23*(7). https://doi.org/10.2196/27633

Lee, K., Liu, Y., Mo, J. Q., Zhang, J., Dong, Z., & Lu, S. (2008). Vav3 oncogene activates estrogen receptor and its overexpression may be involved in human breast cancer. *BMC Cancer*, *8*. https://doi.org/10.1186/1471-2407-8-158

Loibl, S., Poortmans, P., Morrow, M., Denkert, C., & Curigliano, G. (2021). Breast cancer. In *The Lancet* (Vol. 397, Issue 10286, pp. 1750–1769). Elsevier B.V. https://doi.org/10.1016/S0140-6736(20)32381-3

Lyons, L. S., & Burnstein, K. L. (2013). Signaling mechanisms of Vav3, a guanine nucleotide exchange factor and androgen receptor coactivator, in physiology and prostate cancer progression. In *Prostate Cancer: Biochemistry, Molecular Biology and Genetics* (pp. 187–205). Springer New York. https://doi.org/10.1007/978-1-4614-6828-8_6

Matsumoto, A., Jinno, H., Murata, T., Seki, T., Takahashi, M., Hayashida, T., Kameyama, K., & Kitagawa, Y. (2015). Prognostic implications of receptor discordance between primary and recurrent breast cancer. *International Journal of Clinical Oncology*, *20*(4), 701–708. https://doi.org/10.1007/S10147-014-0759-2

Maximov, P. Y., Fan, P., Abderrahman, B., Curpan, R., & Jordan, V. C. (2022). Estrogen Receptor Complex to Trigger or Delay Estrogen-Induced Apoptosis in Long-Term Estrogen Deprived Breast Cancer. *Frontiers in Endocrinology*, *13*. https://doi.org/10.3389/FENDO.2022.869562

Moore, C. B., Guthrie, E. H., Huang, M. T. H., & Taxman, D. J. (2010). Short hairpin RNA (shRNA): design, delivery, and assessment of gene knockdown. *Methods in Molecular Biology (Clifton, N.J.)*, *629*, 141–158. https://doi.org/10.1007/978-1-60761-657-3_10

Nayak, R. C., Chang, K. H., Singh, A. K., Kotliar, M., Desai, M., Wellendorf, A. M., Wunderlich, M., Bartram, J., Mizukawa, B., Cuadrado, M., Dexheimer, P., Barski, A., Bustelo, X. R., Nassar, N. N., & Cancelas, J. A. (2022). Nuclear Vav3 is required for polycomb repression complex-1 activity in B-cell lymphoblastic leukemogenesis. *Nature Communications*, *13*(1). https://doi.org/10.1038/S41467-022-30651-7

Pfaffl, M. W. (2001). A new mathematical model for relative quantification in real-time RT–PCR. *Nucleic Acids Research*, *29*(9), e45. https://doi.org/10.1093/NAR/29.9.E45

Schwartz, A. D., Adusei, A., Tsegaye, S., Moskaluk, C. A., Schneider, S. S., Platt, M. O., Seifu, D., Peyton, S. R., Babbitt, C. C., & Eng, A. B. (2021). *Genetic Mutations Associated with Hormone-Positive Breast Cancer in a Small Cohort of Ethiopian Women HHS Public Access*. *49*(8), 1900–1908. https://doi.org/10.1007/s10439-021-02800-4

Trenkle, T., McClelland, M., Adlkofer, K., & Welsh, J. (2000). Major transcript variants of VAV3, a new member of the VAV family of guanine nucleotide exchange factors. *Gene*, *245*(1), 139–149. https://doi.org/10.1016/S0378-1119(00)00026-3

Tsuboi, M., Taniuchi, K., Furihata, M., Naganuma, S., Kimura, M., Watanabe, R., Shimizu, T., Saito, M., Dabanaka, K., Hanazaki, K., & Saibara, T. (2016). Vav3 is linked to poor prognosis of pancreatic cancers and promotes the motility and invasiveness of pancreatic cancer cells. *Pancreatology*, *16*(5), 905–916. https://doi.org/10.1016/J.PAN.2016.07.002

Uen, Y. H., Fang, C. L., Hseu, Y. C., Shen, P. C., Yang, H. L., Wen, K. S., Hung, S. T., Wang, L. H., & Lin, K. Y. (2015). VAV3 oncogene expression in colorectal cancer: Clinical aspects and functional characterization. *Scientific Reports*, *5*. https://doi.org/10.1038/SREP09360

Wegrzyn, G., & Wegrzyn, A. (2002). Stress responses and replication of plasmids in bacterial cells. *Microbial Cell Factories*, *1*, 2. https://doi.org/10.1186/1475-2859-1-2

Welshons, W. V., & Jordan, V. C. (1987). Adaptation of estrogen-dependent MCF-7 cells to low estrogen (phenol red-free) culture. *European journal of cancer & clinical oncology*, 23(12), 1935–1939. https://doi.org/10.1016/0277-5379(87)90062-9

Winters, S., Martin, C., Murphy, D., & Shokar, N. K. (2017). Breast Cancer Epidemiology, Prevention, and Screening. *Progress in Molecular Biology and Translational Science*, *151*, 1–32. https://doi.org/10.1016/BS.PMBTS.2017.07.002

SUPPLEMENTARY INFORMATION

Supplementary Table 1: classification of the cell lines in our BC panel according to their ER status and intrinsic subtype.

Code	Cell line	ER status	Intrinsic subtype
22	BT-549	Negative	Basal
1	HCC38	Negative	Basal
2	MDA-MB-157	Negative	Basal
3	MDA-MB-231	negative	Basal
4	MDA-MB-231 Brain	Negative (derived from MDA-MB-231)	
5	MDA-MB-231 Bone		
6	MDA-MB-231 Lung		
7	SUM149PT	Negative	Basal
8	HCC1806	Negative	Basal
20	HCC70	Negative	Basal
9	MDA-MB-468	Negative	Basal
10	HCC1569	Negative	Basal
11	HCC1954	Negative	Basal
12	SKBr3	Negative	Luminal
21	MDA-MB-453	Negative	Luminal
13	CAMA-1	positive	Luminal
19	ZR-75-1	Positive	Luminal
14	T47D	Positive	Luminal
15	MCF-7	Positive	Luminal
16	MCF-7-LTED	Positive	Luminal (oestrogen deprivation resistant)
17	BT-474	Positive	Luminal
18	MCF10A (non-tumour breast)	-	-

Supplementary Table 2. Primer sequences used for amplification of *VAV3α*, *VAV3.1*, total *VAV3* and housekeeping genes transcripts by qRT-PCR.

Isoform/gene detected	Forward sequence	Reverse sequence
VAV3α	5'-CGCACTCCATCAACCTGAAG-3'	5'-CCTGATTCCTGTGGCCAATG-3'
VAV3.1	5'-ACTTTACACTGACAATGCCAATT-3'	5'-TCCTTCATGCAGAGCTGGG-3'
Total *VAV3*	5'-AGAGAAACGGACCAATGGACT-3'	5'-GGTGGTGTTCCAGAATAGTTCC-3'
ACTβ	5'-GCAAAGACCTGTACGCCAAC-3'	5'-AGTACTTGCGCTCAGGAGGA-3'
HPRT	5'-TGACACTGGCAAAACAATGCA-3'	5'-GGTCCTTTTCACCAGCAAGCT-3'

Supplementary Table 3. Composition of the buffers employed for experiments.

Buffer	Composition
RIPA lysis buffer	50 mM Tris-HCl pH 7.5, 150 mM NaCl, 1 mM EDTA, 0.1% SDS, 1% NP-40, 1% sodium deoxycholate, 1mM sodium fluoride, 1 mM sodium orthovanadate, 1 mM β-glycerophosphate and protease and phosphatase inhibitor cocktail (phenylmethylsulfonyl fluoride 1nM, aprotinine 10 mg/ml, leupeptin 10 mg/ml and sodium orthovanadate 10 µM).
Protein Loading Buffer	0.313M Tris-HCl (pH 6.8, 25ºC), 10% SDS, 50% glycerol, 5% β-mercaptoethanol and 0'05% (w/v) blue bromophenol.

DNA Loading Dye	10 mM Tris-HCl (pH 7.6), 0.03 % bromophenol blue, 0.03 % xylene cyanol FF, 0.15 % orange G, 60 % glycerol 60 mM EDTA.
Electrophoretic buffer	25 mM Tris, 0.19 M Glycine, 0.1% SDS, water up to volume.
TBST	10% TBS 10x (Tris-buffered saline), 0.1% Tween, water up to volume.
TBE Buffer	89 mM Tris, 89 mM boric acid, 2 mM EDTA, pH ~8.3.

Supplementary Table 4. Vectors selected for VAV3 silencing by shRNA technology and introduced in the lentiviral particles produced.

Commercial clone ID (Sigma-Aldrich)	Target isoform	shRNA target sequence	Vector backbone
TRCN0000047700	VAV3α	5'-CCAATAATCCTACAACCGATA-3'	pLKO.1
TRCN0000047698	VAV3α + VAV3.1	5'-CCGAACTTATTAATAGGGTAA-3'	pLKO.1
TRCN0000047702	VAV3α	5'-CGAAGTTGTTGTCTAGCAGAA-3'	pLKO.1
TRCN0000047699	VAV3α	5'-CGGAACCTAATGCAAGAGATT-3'	pLKO.1
TRCN0000047701	VAV3α + VAV3.1	5'-CCAGTAGATTATTCTTGCCAA-3'	pLKO.1
SHC016-1EA	-	(commercial scramble shRNA sequence)	pLKO.1

Supplementary Figure 1. pLKO.1 vector composition (not all included, only key regulatory elements and elements involved in our experimental approach, including BsaI restriction enzyme cleavage sites).